

大陆板内玄武岩数据挖掘:成分多样性及在判别图中的表现^{*}

王金荣¹ 潘振杰¹ 张旗² 陈万峰¹ 杨婧¹ 焦守涛² 王淑华¹

WANG JinRong¹, PAN ZhenJie¹, ZHANG Qi², CHEN WanFeng¹, YANG Jing¹, JIAO ShouTao² and WANG ShuHua¹

1. 兰州大学地质科学与矿产资源学院,甘肃省西部矿产资源重点实验室,兰州 730000

2. 中国科学院地质与地球物理研究所,北京 100029

1. Key Laboratory of Mineral Resources in Western China (Gansu Province), School of Earth Sciences, Lanzhou University, Lanzhou 730000, China

2. Institute of Geology and Geophysics, China Academy of Sciences, Beijing 100029, China

2015-11-26 收稿, 2016-06-14 改回.

Wang JR, Pan ZJ, Zhang Q, Chen WF, Yang J, Jiao ST and Wang SH. 2016. Intra-continental basalt data mining: The diversity of their constituents and the performance in basalt discrimination diagrams. *Acta Petrologica Sinica*, 32(7):1919–1933

Abstract It is generally considered that continental flood basalts (CFB), rift basalts (CRB), within-plate basalt (WPB) are produced in the plate tectonic setting which is related to the mantle plume activities from the enriched lower mantle, similar to OIB in terms of geochemistry characteristics. In this paper, a GEOROC database of the global CFB, CRB and WPB is used to find that these three categories almost fall in all various basalt tectonic environment areas, some even primarily falls in MORB or IAB, but not in WPB area. This result suggests that the original discriminant function of the basalt discrimination diagrams is still questionable, especially, there exist some problems in most of the discrimination diagrams of continental basalt. All these tremendous changes of CFB, CRB and WPB geochemistry compositions suggest that the source may be strongly heterogeneous: some of CFB, CRB and WPB come from enriched mantle plume with classic characteristics of OIB, some of them derive from MORB source related with the slab-recycled effect, and others from depleted mantle source beneath the island arc lithosphere, characterized by obvious Nb-Ta depletion, similar to island arc basalts. In many places, continental basalts can be divided into two types: low titanium and high titanium. Low-Ti basalts are depleted or strongly depleted, and high-Ti basalts are usually enriched. The study of this paper shows that enriched-type basalts may come from enriched lower mantle, but strongly-depleted-type or depleted-type basalts may derive from the asthenospheric mantle characterized by MORB or IAB. The study further points out that the nature of the source may be the main controlling factor of the qualities of continental basalts. Meanwhile, there are many other important factors leading to the diversity of continental basalts, such as the degree of partial melting, melting depth, fractional crystallization, crustal contamination and AFC process.

Key words Continental flood basalt; Rift basalt; Within-plate basalt; Data mining; Depleted mantle; Enriched mantle; Island arc

摘要 通常认为,大陆溢流玄武岩(CFB)、裂谷玄武岩(CRB)、板内玄武岩(WPB)均产于板内构造环境,其地球化学特征与OIB类似,源于富集的下地幔,与地幔柱的活动有关。本文利用GEOROC数据库对全球CFB、CRB和WPB数据进行挖掘,发现上述三类玄武岩判别图几乎落入了全部的构造环境域,有些甚至主要落入MORB和IAB区,而不是落入WPB区。结果表明原先的玄武岩判别图的判别功能值得商榷,尤其对大陆玄武岩来说,许多判别图都存在问题。全体CFB、CRB和WPB的地球化学成分变化巨大,暗示其源区具有强烈的不均一性:部分CFB、CRB和WPB来自富集的地幔柱,仍然具有经典的OIB的特征;部分来自MORB的源区,与MORB的再循环作用有关;部分来自岛弧岩石圈之下的亏损地幔源区,以强烈亏损Nb-Ta为特征,类似岛弧玄武岩的地球化学特征。许多地区的大陆玄武岩可分为低钛和高钛两类,低钛玄武岩大多是亏损或强烈亏损的,而高钛玄武岩通常是富集型的。本文的研究表明,富集型大陆玄武岩可能来自富集的下地幔,而亏损的和强烈

* 本文受中央高校基本科研业务费项目(Lzu-Jbky-2012-128)及中国地质调查局项目(121201011000150012-02)联合资助。

第一作者简介:王金荣,男,1958年生,教授,博士生导师,岩石大地构造学专业。E-mail: jrwang@lzu.edu.cn

亏损的玄武岩可能来自具有 MORB 或岛弧特征的软流圈地幔。进一步指出,源区性质可能是大陆玄武岩多样性的主控因素,其次为部分熔融程度、熔融深度、结晶分离、陆壳混染以及 AFC 过程。

关键词 大陆溢流玄武岩;裂谷玄武岩;板内玄武岩;数据挖掘;亏损地幔;富集地幔;岛弧

中图法分类号 P581; P588. 145

1 引言

大陆溢流玄武岩是大陆上分布广,研究最详细的玄武岩类,巨大规模的大陆溢流玄武岩被称为大火成岩省,如北大西洋第三纪玄武岩、德干高原玄武岩、Parana 玄武岩、峨眉山玄武岩等。裂谷玄武岩、板内玄武岩的规模稍逊于大陆溢流玄武岩,尤其东非裂谷玄武岩,被视为板块扩张的初始阶段而备受学术界重视。20世纪70~80年代,以 Pearce 首领的一批学者 (Pearce, 1975, 1976, 1982, 1983; Pearce and Robinson, 2000; Pearce and Cann, 1973; Pearce and Gale, 1977; Pearce and Norry, 1979; Pearce and Peate, 1995; Pearce *et al.*, 1984; Capedri *et al.*, 1980; Glassley, 1974; Harris *et al.*, 1986; Meschede, 1986; Mullen, 1983; Wood *et al.*, 1979; Wood, 1980; Galoyan *et al.*, 2007; Workman and Hart, 2005) 致力于玄武岩构造判别图的构建,为板块构造和大陆造山带研究开辟了新的途径,极大地丰富了玄武岩研究的内容,将玄武岩构造环境及其形成的地球动力学过程的研究推向了高峰。然而,随着地球科学技术及仪器设备的发展,全球火成岩数据库的积累及应用,地质科学家对原先建立起来的玄武岩判别图进行了重新评估,发现其判别功能存在诸多缺陷,并初步提出了修正路径 (Li *et al.*, 2015; Vermeesch, 2006a, b; Snow, 2006)。

本文利用 GEOROC 数据库资料,对全球大陆溢流玄武岩、裂谷玄武岩和板内玄武岩数据进行了初步的挖掘,发现早先的玄武岩构造环境判别方法的理论和思路可能存在一些问题。早先的判别图由于时代、研究区域、研究思路以及研究手段和分析技术的限制,得出的结论或者取得的认识必然具有一定的局限性,或存在某些不足的。之前认为,大陆溢流玄武岩、裂谷玄武岩和板内玄武岩是来自于富集的下地幔,而通过对全球大陆溢流玄武岩、裂谷玄武岩和板内玄武岩的数据挖掘、研究发现,多数的样品并非是强烈富集的,部分样品甚至是亏损的,陆内玄武岩地球化学特征及性质具有明显的多样性。因此,利用 GEOROC 数据库对大陆溢流玄武岩、裂谷玄武岩、板内玄武岩进行数据挖掘,探究陆内玄武岩的源区性质以及构造判别图的可信度、选择可信的判别元素具有重要的科学意义。本文仅为数据挖掘的尝试性研究,旨在抛砖引玉的作用。

2 研究方法

数据筛选是研究的前提,虽然耗时多,但对保证结果的

精确性和可靠性至关重要。在数据分析过程中如发现问题需重新筛选。筛选数据必须客观,切忌主观臆测。

2.1 数据筛选的原则和主要内容

1)剔除超镁铁岩、侵入岩、中酸性岩、辉长岩等的数据,仅保留玄武岩、辉绿岩和粒玄岩的数据;2)剔除 $\text{SiO}_2 < 45\%$ 和 $\text{SiO}_2 > 55\%$ 的数据,剔除非玄武岩样品;3)剔除 $\text{TiO}_2 < 0.1\%$ 的样品,个别玄武质玻璃会出现这种情况;4)剔除 $\text{Mg}^{\#} > 0.70$ 的样品,根据不同作者的研究,玄武岩原始岩浆的 $\text{Mg}^{\#}$ 大体在 0.65~0.72 之间,大于该数值的样品即为堆晶岩,堆晶岩不能判别构造环境;5)剔除 $\text{Al}_2\text{O}_3 < 10\%$ 和 $\text{Al}_2\text{O}_3 > 18\%$ 的样品,个别玄武质玻璃会出现这种情况;6)剔除烧失量和 $\text{H}_2\text{O} > 7\%$ 、 $\text{CO}_2 > 3\%$ 的数据,挥发分和 H_2O 含量高,指示蚀变作用强烈; CO_2 含量高,指示碳酸盐化、方解石化强烈;7)剔除 $\text{K}_2\text{O} > 8\%$ 、 $\text{Na}_2\text{O} > 10\%$ 和 $\text{CaO} > 20\%$ 的样品,防止其它类型的样品混入;8)其他可能发生的分析错误的数据,例如某些元素含量比大多数数据低 1~2 个数量级的数据;9)剔除个别数据库本身错误的数据。我们在数据筛选过程中,发现有一批数据类似岛弧或者弧后的特征 (Wang *et al.*, 2007; Maxeiner *et al.*, 2005; Rogers *et al.*, 2006; Dunning *et al.*, 1991; Greene *et al.*, 2009),通过查看原始文献,发现原作者研究的确实为岛弧或者数据所在位置确为岛弧,推测可能是数据录入时误将其列入板内玄武岩。

2.2 作图

1)区分大陆溢流玄武岩、裂谷玄武岩、板内玄武岩,考察它们之间是否存在差异,及其在判别图中的分布;2)查阅判别图原始文献,了解判别图的数据来源、原作者的思路和结论;3)对比本次研究,得出相应的结论。

2.3 样品分布

筛选后全部大陆溢流玄武岩(CFB)、裂谷玄武岩(CRB)、板内玄武岩(WPB)样品在全球范围内的分布(图 1)。

2.4 数据来源与数据量

本文是根据 GEOROC 数据库的资料进行研究的。通过对筛选后的全部数据进行整理,统计了大陆溢流玄武岩(CFB)、裂谷玄武岩(CRB)、板内玄武岩(WPB)的数据来源和数据量(表 1)。CRB 和 CFB 是 GEOROC 数据库中固有的分类,而数据库中的 WPB 据我们推测可能是除了 CRB 和 CFB 之外的具板内玄武岩地球化学特征的大陆玄武岩。

表 1 全部 CFB、CRB、WPB 样品的数据来源与数据量统计表

Table 1 The statistical chart of data sources and data volume of all the CFB, CRB and WPB samples

大陆溢流玄武岩(CFB)	n	板内玄武岩(WPB)	n
AUSTRALIA	175	ADRIA DOMAIN	22
EMEISHAN	443	AMAZONIAN CRATON_PROTEROZOIC	66
CENTRAL ATLANTIC MAGMATIC PROVINCE	969	AMUR SUPERTERRANE	21
CHIFENG FLOOD BASALTS	30	ANATOLIA-IRAN BELT-CENOZOIC/QUATERNARY	1485
CHILCOTIN PLATEAU BASALTS/BRITISH COLUMBIA	44	ANDEAN BASINS-MESOZOIC	154
DECCAN	2043	ANTARCTICA-PALEOZOIC	83
ETENDEKA PROVINCE	473	ANTARCTICA/PATAGONIA-MESOZOIC	152
FRANKLIN LARGE IGNEOUS PROVINCE	34	ARABIAN-NUBIAN SHIELD-CENOZOIC	754
HIGH ARCTIC LARGE IGNEOUS PROVINCE	136	ARABIAN-NUBIAN SHIELD-MESOZOIC	62
HURONIAN FLOOD BASALT PROVINCE	76	ARABIAN-NUBIAN SHIELD-NEOPROTEROZOIC	339
KAROO AND FERRAR PROVINCES	1433	ARAVALI CRATON_PROTEROZOIC	7
KUZNETSK BASIN (KUZBASS) TRAPS	13	ARGENTINA-PALEOZOIC	12
MACKENZIE LARGE IGNEOUS PROVINCE	211	ATLAS MOUNTAINS	76
MADAGASCAR FLOOD BASALT	224	AUSTRALIA	1378
MARATHON LARGE IGNEOUS PROVINCE	60	BAIKAL RIFT ZONE_CENOZOIC	240
MIDCONTINENT RIFT SYSTEM-KEWEENAWAN	220	BAIKAL-PATOM REGION_PROTEROZOIC	58
NANDALING-YANSHAN BELT	17	BALTIC SHIELD-PALEOZOIC	21
NILUFER UNIT-YENISEHIR ASSOCIATION-PONTIDES	22	BALTIC SHIELD-PROTEROZOIC	788
NORTH ATLANTIC IGNEOUS PROVINCE (NAIP)	2106	BASTAR CRATON_MESOZOIC	1
PANJAL TRAP	50	BERING SEA BASALT PROVINCE-CENOZOIC	7
PARANA	1021	BIRIMIAN-WEST AFRICA	196
RAJAHMUNDY TRAPS	26	CANADIAN SHIELD_MESOZOIC	2
RAJMAHAL-BENGAL-SYLHET	119	CANADIAN SHIELD_PALEOZOIC	4
SIBERIAN TRAPS	472	CANADIAN SHIELD_PROTEROZOIC	154
SOUTH TETHYAN SUTURE ZONE-PAKISTAN	6	CARPATHIAN BELT AND PANNONIAN BASIN	687
UMKONDO PROVINCE	10	CAUCASUS	51
TARIM BASIN	79	CENTRAL AFRICAN REPUBLIC	8
VILUY TRAPS	14	CENTRAL ASIAN FOLDBELT-CENOZOIC	2940
WRANGELLIA	184	CENTRAL ASIAN FOLDBELT-MESOZOIC	1111
YELLOWSTONE-SNAKE RIVER PLAIN VOLCANIC PROVINCE	3019	CENTRAL ASIAN FOLDBELT-PALEOZOIC	1325
YEMEN PLATEAU	94	CENTRAL ASIAN FOLDBELT-PROTEROZOIC	741
裂谷玄武岩(CRB)	n	CENTRAL-EAST IRANIAN MICROCONTINENT	24
ANTARCTICA	250	CIRCUM-PARANA ALKALINE VOLCANIC PROVINCES-CENOZOIC	22
APPALACHIANS	615	CIRCUM-PARANA ALKALINE VOLCANIC PROVINCES-MESOZOIC	191
AUSTRALIA	13	COLORADO PLATEAU	164
BASIN AND RANGE-GREAT BASIN	823	DARFUR DOME VOLCANIC PROVINCE SUDAN	112
EAST AFRICAN RIFT	1308	DINARIDES	20
GARDAR PROVINCE-GREENLAND	53	EAST SAHARA SWELL-CRETACEOUS	27
GULF OF SUEZ RIFT	13	EASTERN MEDITERRANEAN BELT-CENOZOIC	57
LATE CRETACEOUS IBERIAN IGNEOUS PROVINCE	2	EASTERN MEDITERRANEAN BELT-MESOZOIC	166
MEXICAN BASIN AND RANGE	469	ETHIOPIAN PLATEAU	29
MID-AFRICAN RIFT SYSTEM	283	EUROPEAN OROGENIC BELT-CENOZOIC	1091
NORTHERN VARISCAN FORELAND	19	EUROPEAN OROGENIC BELT-MESOZOIC	11
OMAN RIFT	28	EUROPEAN OROGENIC BELT-PALEOZOIC	648
OSLO RIFT	20	EUROPEAN OROGENIC BELT-PROTEROZOIC	6
RED SEA RIFT	128	GUYANA SHIELD-PROTEROZOIC	7
RIO GRANDE RIFT	216	HOGGAR SWELL	40
ROSS OROGEN-TRANSANTARCTIC MOUNTAINS-CAMBRIAN	6	KAAPVAAL CRATON_MESOZOIC	5
SICILY CHANNEL RIFT	136	KAAPVAAL CRATON_PROTEROZOIC	24
SIRTE BASIN	6	KOHISTAN-LADAKH TERRANE (GANGDISE BELT)	146
SORGENDREI-TORNQUIST ZONE-NORTH SEA VOLCANIC PROVINCE	98		

续表 1

Continued Table 1

MACKENZIE LARGE IGNEOUS PROVINCE	5	RIO DE LA PLATA CRATON	81
MADAGASCAR-CENOZOIC	34	SAO FRANCISCO CRATON_PROTEROZOIC	17
MADAGASCAR FLOOD BASALT	2	SOUTHERN PATAGONIA	10
MESETA DE CANQUEL	10	SUL RIO GRANDENSE SHIELD_PROTEROZOIC	27
MIDCONTINENT US KIMBERLITE-CARBONATITE PROVINCE	3	TOCANTINS PROVINCE	32
MUNSTER BASIN	10	TRANS-HUDSON OROGEN	239
NAMAQUALAND NATAL BELT_PROTEROZOIC	26	UKRAINIAN SHIELD	2
NEW ZEALAND	914	URALS	46
NORTH AMERICAN CORDILLERA-CENOZOIC-QUATERNARY	746	VERKHOYANSK-CHUKOTKA COLLISION ZONE	6
NORTH AMERICAN CORDILLERA-MESOZOIC	177	WEST-AFRICAN COASTAL BELTS-PAN-AFRICAN	14
NORTH AMERICAN CORDILLERA-PALEOZOIC	153	WYOMING CRATON_CENOZOIC	42
NORTH ATLANTIC CRATON_PROTEROZOIC	115		

注:据 GEOROC 数据库,阿拉伯数字为本文采用的经过数据筛选后的样品数量

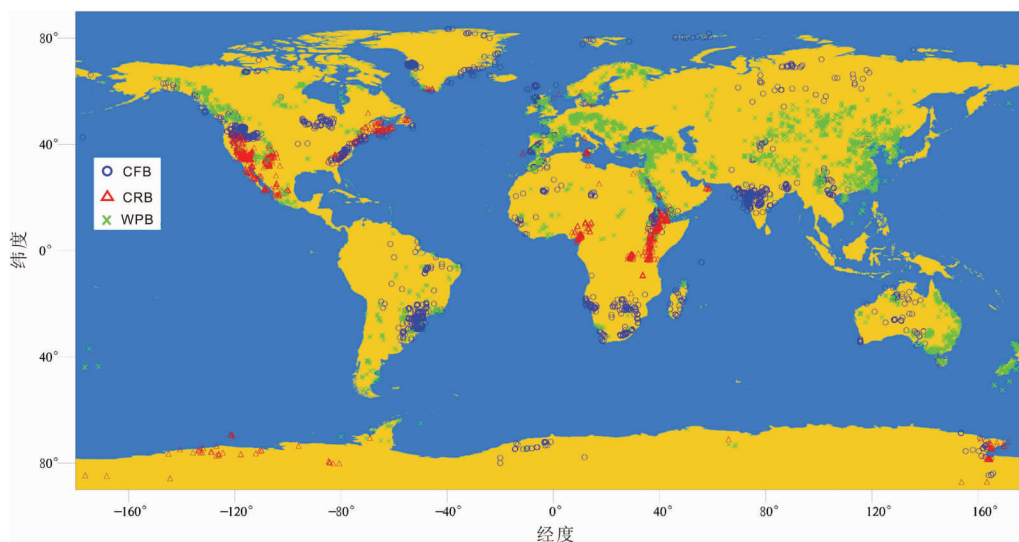


图 1 全部的 CFB、CRB、WPB 样品在全球的分布(据 GEOROC 数据库)

CFB-大陆溢流玄武岩;CRB-大陆裂谷玄武岩;WPB-板内玄武岩(下同)

Fig. 1 Distribution of all the CFB, CRB and WPB samples in the world (after GEOROC Database)

CFB-Continental Flood Basalts; CRB-Continental Rift Basalts; WPB-Within-Plate Basalts (the same below)

3 玄武岩判别图

本次研究采用的 GEOROC 数据库的数据总共 113614 个, 经过筛选淘汰数据 76313 个, 留下的有效数据 37331 个。其中大陆溢流玄武岩 14287 个, 裂谷玄武岩 4499 个, 板内玄武岩 18545 个。全部数据中, 全岩数据 36693 个, 玻璃 638 个。玻璃与全岩一样适合用于构造环境判别。我们对全部全岩与玻璃样品进行投图, 结果表明, 在数据筛选之后, 全岩和玻璃的地球化学性质大体是相当的, 投图得出的结果也大体是一致的(限于篇幅, 文中未列该图)。

(1) $\text{FeO}^T\text{-MgO-Al}_2\text{O}_3$ 图(图 2a)。该图是 Pearce 和 Gale (1977) 设计的, 使用了 8400 个数据(包括 1003 个大陆

玄武岩的数据)。本文使用了 14237 个大陆溢流玄武岩数据、4329 个裂谷玄武岩数据、5090 个板内玄武岩数据, 在该判别图上, 样品几乎落入了判别图中各种不同的环境域, 说明该图的判别功能还存在问题。从图 2a 中可以看出, 大陆溢流玄武岩、裂谷玄武岩和板内玄武岩样品的分布范围较一致, 并无明显差别。不同的是 WPB 具富铝的趋势。通常认为, 典型的板内玄武岩是贫铝的, 岛弧玄武岩(图 2a 中的造山带范围)是富铝的(Pearce *et al.*, 1984)。

(2) Ti-Zr-Y 图(图 2b)。该图是 Pearce 和 Cann (1973) 提出来的。一共使用了 200 多个样品, 包括大陆裂谷玄武岩 35 个。原作者认为, 该图最大的优点是能够正确区分板内玄武岩与来自洋中脊和岛弧的玄武岩。Pearce *et al.* (1984) 强调该图区分上述玄武岩的有效率可高达 95% 以上, 认为是地幔不均一性的反映。本次研究使用的 11018 个

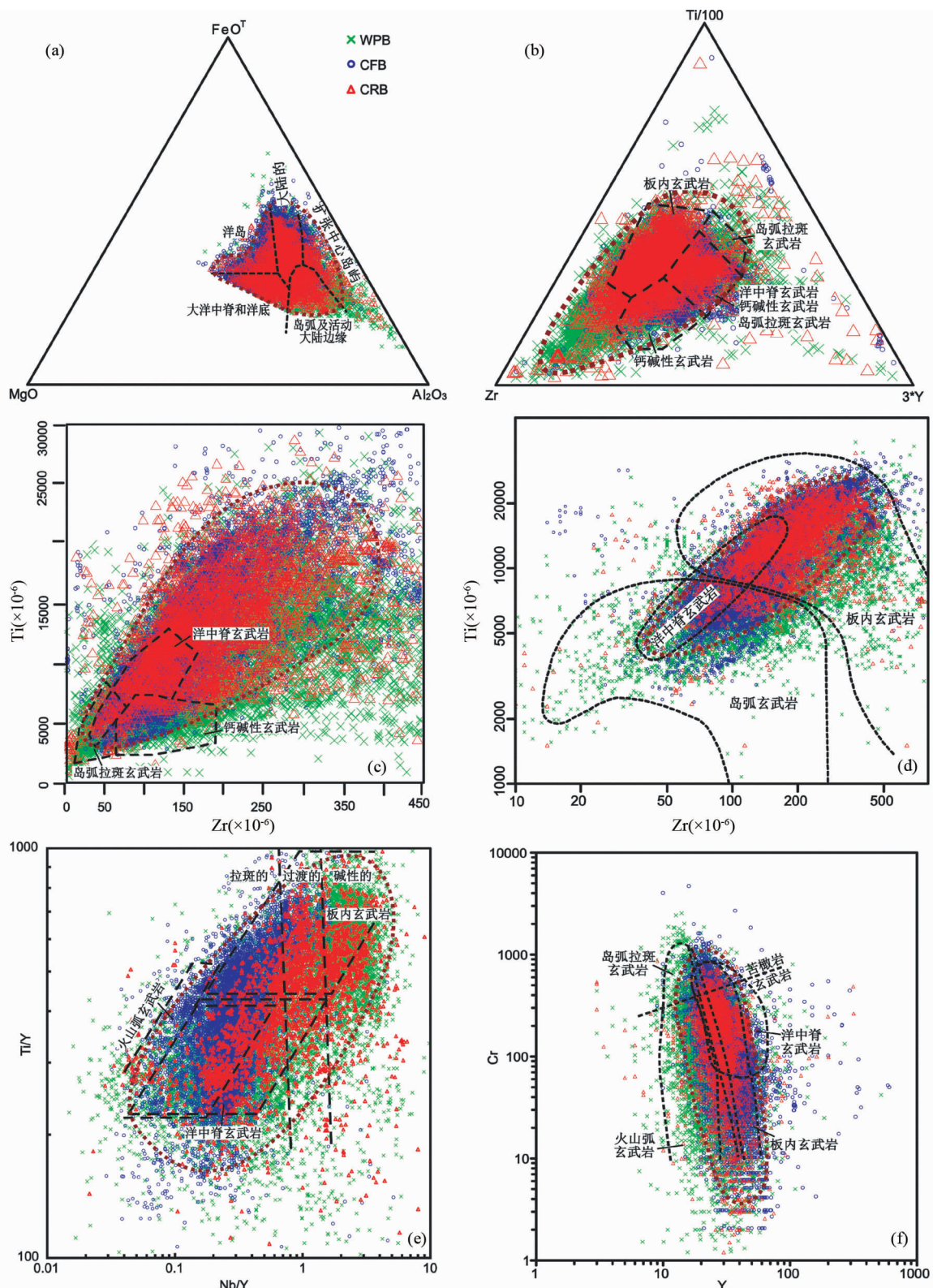


图2 全部 WPB、CFB 和 CRB 样品判别图解

粗棕色点线圈定的是 WPB、CFB 和 CRB 数据的共同密集区(下同)

Fig. 2 All the samples of WPB, CFB and CRB discrimination diagrams

The common dense areas of WPB, CFB and the CRB data is circled by thick brown line (the same below)

大陆溢流玄武岩数据、2980个裂谷玄武岩数据、11654个板内玄武岩数据,也几乎覆盖了所有的构造环境域,提示Pearce *et al.* (1984)对该图的评价值得商榷。值得注意的是,有相当多的数据超出了判别图的范围,尤其是板内玄武岩,Zr的含量很高,数据向Zr端元汇集。

(3) Ti-Zr图(图2c, d)。这个图最初是由Pearce and Cann (1973)提出来的,后来Pearce又于1981和1982年对其作了修正(Pearce *et al.*, 1981; Pearce, 1982)。图2c, d使用了11513个大陆溢流玄武岩数据、3335个裂谷玄武岩数据、12291个板内玄武岩数据,样品投入所有的玄武岩构造环境域,样品的分布几乎与MORB范围完全重叠,许多数据已远远超出了原判别图的范围,无法区分OIB、MORB和IAL(岛弧熔岩)。

(4) Ti/Y-Nb/Y图(图2e)。该图是Pearce于1982年提出(Pearce, 1982),1984年修改的(Pearce *et al.*, 1984b)。原作者认为,Ti/Y是区分板内玄武岩与其他类型玄武岩最好的标志。但是,通过对5304个大陆溢流玄武岩、1778个裂谷玄武岩、8783个板内玄武岩数据投图,发现样品的分布范围几乎包括了判别图中的所有区域,提示此图判别板内玄武岩与其他类型玄武岩的方法也存在问题。

(5) Cr-Y图(图2f)。该图是Pearce于1981, 1982年提出来的(Pearce *et al.*, 1981; Pearce, 1982),认为该图主要用以区分岛弧和非岛弧玄武岩。从10005个大陆溢流玄武岩、2637个裂谷玄武岩、9982个板内玄武岩数据投图结果来看,其判别功能也失去了效果。王金荣等(待刊)的研究表明,MORB和OIB基本上不落在岛弧区域,暗示MORB和OIB富Y而岛弧贫Y。在图2f中有不少板内玄武岩样品落入了岛弧域,说明板内玄武岩Y、Cr含量变化大,相当一部分贫Cr的样品超出了原判别图的范围(图2f)。

(6) Hf-Th-Nb图(图3a, Wood, 1980)。该图的最大特色是利用岛弧玄武岩Th>Ta的特征,区分岛弧和非岛弧的玄武岩(Wood, 1980)。本文的4492个大陆溢流玄武岩、1479个裂谷玄武岩、7890个板内玄武岩数据投图,CFB、CRB、WPB的密集区域涵盖了所有的构造环境区域。值得指出的是,上述玄武岩有相当一部分的Th/Ta比值是大于3,类似岛弧的特征,其原因我们将在后面详细讨论。

(7) Nb-Zr-Y图(图3b, Meschede, 1986)。该图是基于NMORB、P-MORB、WPT、WPA四种类型的样品数据共1847个而设计的。本文采用的9993个大陆溢流玄武岩、2816个裂谷玄武岩、11420个板内玄武岩数据投图,样品落入全部的构造环境域,可见该图的判别功能值得讨论。

(8) Zr/Y-Zr图(图3c, Pearce and Norry, 1979)。该图可鉴别岛弧(或火山弧)玄武岩、MORB和板内玄武岩(邓晋福等, 2015)。原作者将Zr/Y=3作为区分板内玄武岩与非板内玄武岩的界线(Pearce, 1983; Rollison, 1993)。我们将本次研究的11025个大陆溢流玄武岩、2981个裂谷玄武岩、12043个板内玄武岩数据投图,样品大部分进入板内玄武岩

区域,部分进入MORB和岛弧区。

(9) Th/Yb-Ta/Yb图(图3d, Pearce, 1982)。该图主要根据岛弧和非岛弧Th/Ta比值的差异设计的。我们使用4678个大陆溢流玄武岩数据、1596个裂谷玄武岩数据、7512个板内玄武岩数据的投图表明,大部分样品落入了VAB区域,只有部分样品落入WPB区,说明该图在设计时存在明显缺陷。

(10) Y-La-Nb图(图3e, Cabanis and Lecolle, 1989)。按照该图的设计,CFB、CRB、WPB应该落入2A和3A区。本文研究的7450个大陆溢流玄武岩、2266个裂谷玄武岩、9861个板内玄武岩数据进行投图,虽然CFB、CRB、WPB样品的主要密集区域在2A、2B、3A区域,但仍有不少数据落入火山弧区和弧后区,说明该图也存在较多问题。

(11) Ti-V图(图3f, Shervais, 1982)。Shervais(1982)用Ti/V值来区分IAT、MORB和OIB。本文将9612个大陆溢流玄武岩、2423个裂谷玄武岩、9764个板内玄武岩数据投入该图,多数落入MORB区域,部分投入岛弧和OIB区域,提示该图的判别功能也存在问题。

4 讨论

(1) 上述研究表明,大陆溢流玄武岩、裂谷玄武岩和板内玄武岩有很宽的成分变化范围,几乎覆盖了判别图上全部的构造环境域,说明这些判别图的判别功能存在明显的缺陷,急需对此作出重新评价。为什么会出现这种情况?可能是由于受二十世纪研究技术、条件以及学术思想的限制,特别是当时设计玄武岩判别图时采用的数据量较少或者只是采用具有典型性的数据。我们采用全体数据投图,避免了“典型”与抽样的缺陷,因而得出的认识应该是真实的、科学的。最近,Li *et al.* (2015)利用GEOROC数据库资料检查了不同构造环境下玄武岩(大陆溢流玄武岩、洋中脊玄武岩、洋岛玄武岩、大洋高原玄武岩、弧后盆地玄武岩及各种类型的弧玄武岩)的Zr、Ti、V、Y、Th、Hf、Nb、Ta、Sm和Sc判别图,发现不同类型的玄武岩之间的重叠区域太大,在所检查的判别图中,没有一个判别图能够清楚地区分开弧后盆地玄武岩和洋中脊玄武岩、大陆溢流玄武岩、洋底高原玄武岩以及其它不同类型的火山弧玄武岩(洋内弧,岛弧和陆缘弧),这与本文的见解基本一致。

(2) 在有些判别图中,上述玄武岩大部分不是落入OIB区,而是进入IAT和VAB区(如Hf-Th-Nb图(图3a)、Nb-Zr-Y图(图3b)、Th/Yb-Ta/Yb图(图3d)、Y-La-Nb图(图3e))。在图3A中,裂谷玄武岩(CRB)大多落入WPB区,表明CRB的源区可能主要是来自下地幔,是相对富集的,而大陆溢流玄武岩和板内玄武岩(CFB和WPB)样品大部分不在WPB区,而是进入MORB和岛弧区,暗示CRB与后两类玄武岩的源区可能有区别,也可能后两类玄武岩与MORB发生过混合作用(数据进入MORB域)或受到过更多的陆壳混染作用的影响(数据进入岛弧域)。当然,玄武岩地幔源区高度不均一

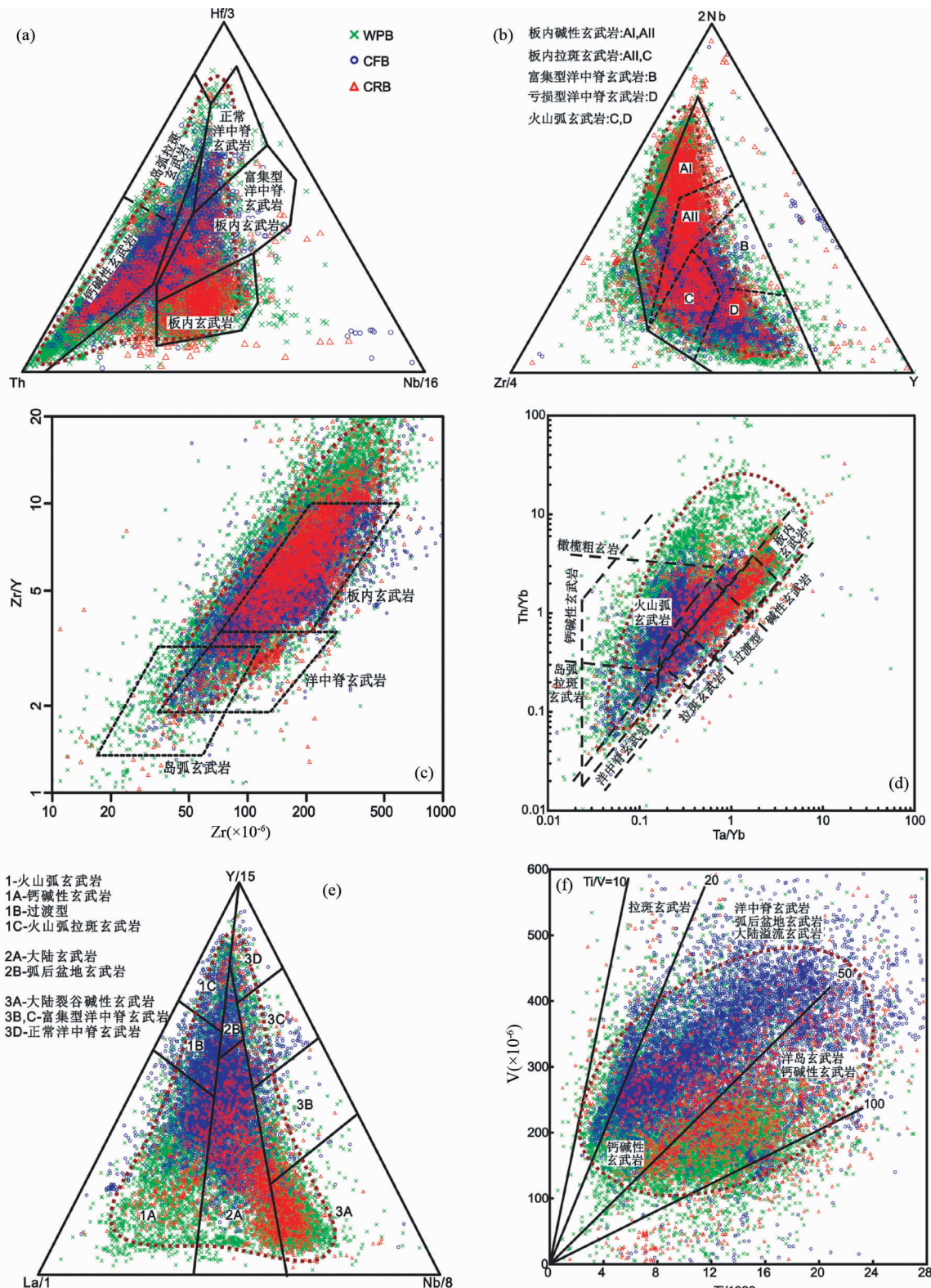


图3 全部 WPB、CFB 和 CRB 样品判别图解

Fig. 3 All the samples of WPB, CFB and CRB discrimination diagrams

性也可能是一个重要的原因。图3d的WPB区域范围很小，分布在 $\text{Th}/\text{Yb} > 3$ 和 $\text{Ta}/\text{Yb} > 3$ 的区域，上述产于大陆内部的

玄武岩大多投入MORB、岛弧和陆缘弧区，较少进入WPB区。我们怀疑该图在设计时是否存在某种缺陷，或者大陆内玄

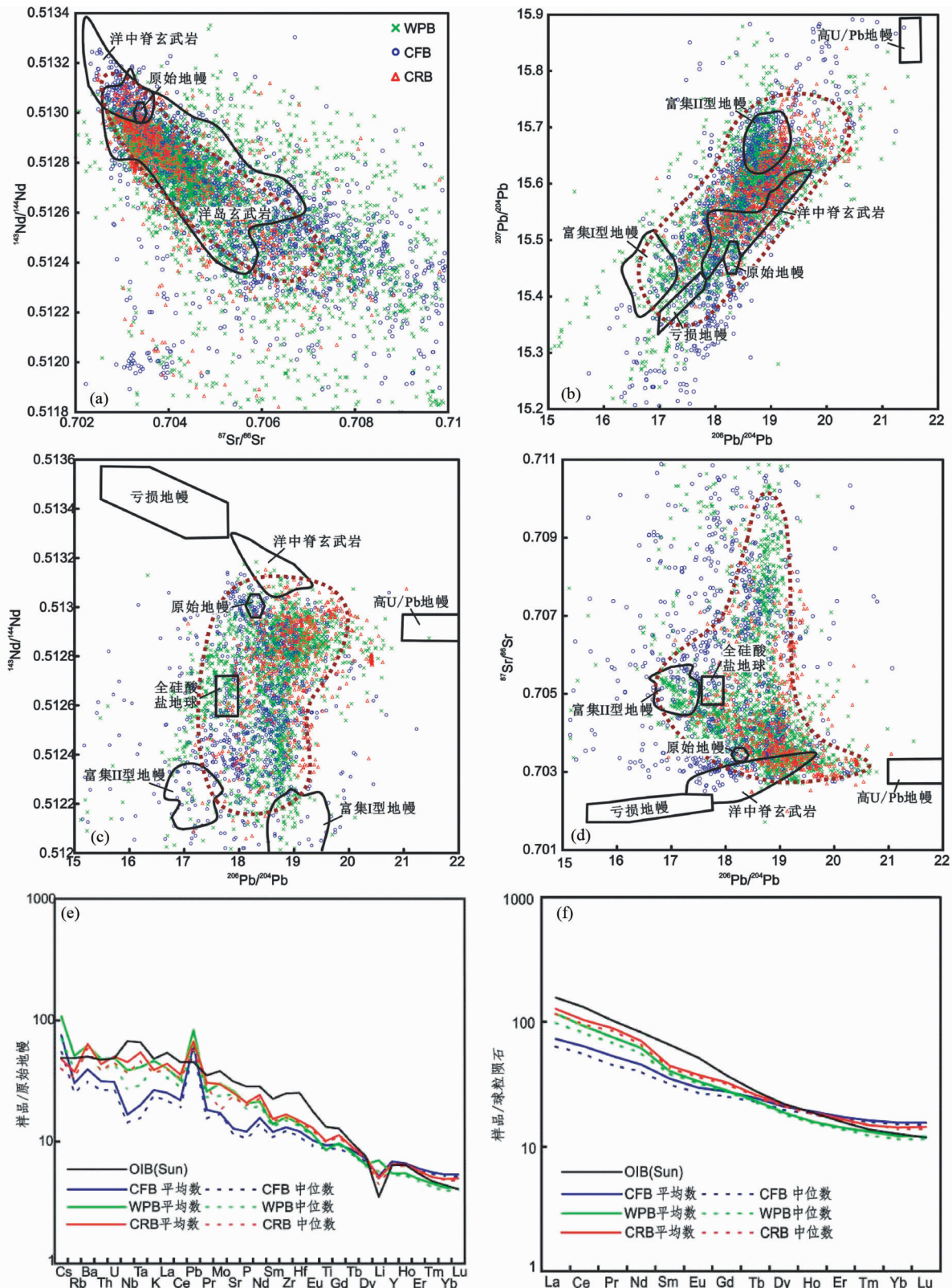


图4 全部WPB、CFB和CRB样品的Nd-Sr-Pb同位素图(a-d)及平均值微量元素原始地幔标准化蛛网图(e)和稀土元素球粒陨石标准化配分图(f)(标准化值据Sun and McDonough, 1989)

Fig. 4 Nd-Sr-Pb isotopic diagrams (a-d), and primitive mantle-normalized trace element patterns (e) and chondrite-normalized REE patterns (f) (normalization values after Sun and McDonough, 1989) of all the WPB, CFB and CRB samples

武岩源区具有多样性, 才导致 WPB 样品不落入 WPB 区域的情况。

(3) 按照早先的认识, CFB、CRB、WPB 基本上属于 OIB 类, 必然覆盖 OIB 区域, 许多判别图确实如此。从 $^{143}\text{Nd}/^{144}\text{Nd}$ - $^{87}\text{Sr}/^{86}\text{Sr}$ 图(图 4a)看, CFB、CRB、WPB 的样品覆盖了原始地幔(PM)和 OIB 的几乎全部范围, 显示其源区富集的特征。在 $^{207}\text{Pb}/^{204}\text{Pb}$ - $^{206}\text{Pb}/^{204}\text{Pb}$ 图(图 4b)中, 全部样品大体在富集端元 EMII 和原始地幔(PM)的范围内, 也有相当一部分样品落在 Zindle and Hart (1986) 的 MORB 范围, 相对于 $^{207}\text{Pb}/^{204}\text{Pb}$ 来说, $^{206}\text{Pb}/^{204}\text{Pb}$ 的比值略高, 也指示了源区地幔富集 $^{206}\text{Pb}/^{204}\text{Pb}$ 的特征。在图 $^{143}\text{Nd}/^{144}\text{Nd}$ - $^{206}\text{Pb}/^{204}\text{Pb}$ (图 4c) 和图 $^{87}\text{Sr}/^{86}\text{Sr}$ - $^{206}\text{Pb}/^{204}\text{Pb}$ 图(图 4d) 中, 富集特征更加明显, 绝大部分样品投到了(原始地幔)PM 和(全硅酸盐地球)BSE 的范围内, 部分投入 EMII 的范围内。陆内玄武岩同位素地球化学特征总体表现为富集的特征。

(4) 本文将所研究的玄武岩分析数据进行系统的数据统计, 包括平均值和中位数两个指标(表 2), 其列出了全部的 CFB、CRB、WPB 的氧化物、微量元素、稀土元素和同位素的数据量、平均值、中位数、众数和含量范围。由于数据库给出的数据不全, 对个别含量甚微的元素, 同时计算了平均值、中位数和众数值。从表 2 和图 4e, f 可以看出, 如果平均值和中位数值相差不大, 平均值是可信的; 个别元素二者相差较大, 如全体 WPB 的 Rb 和 Ba 含量, 平均值和中位数分别为 32.20、25.09 和 435、368, 暗示部分样品缺失数据。这时, 中位数可能是相对可信的, 而平均值可能偏高了。众所周知, Sun and McDonough (1989) 在 Wood *et al.* (1979) 依据元素相容性排序建立的蜘蛛网图的基础上, 进行了全面总结及机制解释, 并从地幔地球化学研究角度, 提出了微量元素标准化值和微量元素原始地幔标准化蛛网图, 使这一图件更加规范, 并得到了学术界的广泛引用。本文统计的数据资料(表 2), 与原作者建立的图的基本样式是一致的。但是, 元素含量具有明显的变化(图 4e, f)。图 4e 显示, 本文统计的 CRB 大离子亲石元素平均值相对于 Sun and McDonough (1989) 的 OIB 平均值略亏损, 而高场强元素则变化不大。说明 CRB 并不像早先认为的 LREE 和 HREE 都是强烈分离的, 而有相当一部分 CRB 是具有 MORB(主要是 E-MORB)的特征, 少量 CRB 表现为相对亏损, 因此 CRB 的大离子亲石元素的平均值和中位数略降低。这可能代表了全球各种各样的 CRB 特征, 而不仅仅是典型的大陆裂谷玄武岩的地球化学特征。此外, 本文统计的 WPB、CFB 和 CRB 与 Sun and McDonough (1989) 的 OIB 比较, 明显富集 Pb, 这是因为 OIB 处于洋壳内部, 不受陆壳的影响, 因而 Pb 含量是较低, 而大陆玄武岩很难避免陆壳混染的影响, 因为陆壳微量元素中最明显的特征之一就是富集 Pb; Nb 和 Ta 表现为相对亏损。

对于大陆溢流玄武岩 Pb 富集和 Nb、Ta 亏损的地球化学特征, 学术界通常有以下一些解释:(1)来自具有上述地球化学特征的地幔柱(Wilson, 1997);(2)受到地幔柱和陆壳岩

浆的混染(Arndt *et al.*, 1993);(3)OIB 或软流圈熔体与过碱性的镁铁质岩浆(钾镁煌斑岩, 金伯利岩)的混合, 后者来自交代的岩石圈地幔, 可能随后还受到陆壳的混染(Arndt and Christensen, 1992; Gibson *et al.*, 2006; Heinonen *et al.*, 2010);(4)来自洋底高原玄武岩(OPB 型)(Kerr and Mahoney, 2007);(5)OIB, MORB 与 SCLM(大陆下岩石圈地幔)有关的熔体的三元混合, 可能随后有陆壳混染;(6)来自富集不相容元素的(如交代的 SCLM)浅部源区的熔融或消减带之上地幔楔的部分熔融(Puffer, 2001; DeMin *et al.*, 2003; Deckart *et al.*, 2005; Dorais and Tubrett, 2008)。由此可见, 大陆溢流玄武岩亏损 Nb-Ta 的原因是比较复杂的。

(5) CRB 与 CFB 存在明显的差别(图 4e)。与 CRB 相比, CFB 相对富 SiO₂, 通常认为是 CFB 受到陆壳混染导致的(Best and Christiansen, 2001), CRB 的 Th/Ta(3.46)比值大于 CFB 的 Th/Ta 比值(1.72)即是证明(见表 2)。但是, CFB 的 K₂O 含量(0.70%)比 CRB(1.1%)的低(见表 2), 似乎与陆壳混染作用相背离, 其原因可能与裂谷玄武岩部分熔融程度较低有关。CRB 的 P₂O₅ 含量(0.43%)高于 CFB(0.23%)也可以用部分熔融程度的不同来解释。此外, CRB 比 CFB 更加富集大离子亲石元素(Ba、Th、U、Nb、Ta、La 以及 Sr、Nd、Pb 同位素等, 见表 2), 也与 CRB 部分熔融程度相对较低相一致(Best and Christiansen, 2001)。

(6) 贫 Ti 大陆溢流玄武岩。大陆溢流玄武岩往往出现高钛和低钛两类玄武岩, 张招崇等(2001)总结了其成因主要有:(1)上升的地幔柱不同部位的部分熔融(Campbell and Griffiths, 1990; Arndt *et al.*, 1993)或岩石圈地幔与软流圈组分不同程度的混合(Piccirillo *et al.*, 1989; Hawkesworth *et al.*, 1988; Peate and Hawkesworth, 1996)并受到不同程度的地壳混染(Hawkesworth *et al.*, 1988; Petrini *et al.*, 1987);(2)不均匀的陆下岩石圈地幔(SCLM)由于地幔柱的加热作用在“湿”的条件下发生熔融(Gallagher and Hawkesworth, 1992, 1994);(3)来自地幔柱的苦橄质岩浆在上升过程中通过 SCLM 时与镁质超钾质岩浆(钾镁煌斑质)发生不同程度的混合(Gibson *et al.*, 1996; Ellam and Cox, 1991; Luttinen and Furnes, 2000);(4)来自地幔柱的 MORB 型拉斑质苦橄岩浆与来自 SCLM 的高 Ti 和低 Ti 钾质熔体混合, 之后又受到地壳的混染(Gibson *et al.*, 1995)。

著名的 Karoo 大火成岩省玄武岩具有低钛和高钛两类, 二者均具有 Nb-Ta 负异常和 Sr-Nd-Pb 同位素富集的特征(Cox *et al.*, 1967; Hawkesworth *et al.*, 1984; Ellam and Cox, 1991; Marsh *et al.*, 1997; Elburg and Goldberg, 2000; Eglington *et al.*, 1989; Huang *et al.*, 1995; Cornell *et al.*, 1996; Eglington and Armstrong, 2003; Kampunzu *et al.*, 2003; Lana *et al.*, 2004), 被解释为来自岩石圈之下的 MORB 或 OIB 地幔源区的岩浆在深部地壳经历了混染、分离结晶和 AFC 过程, 导致具有明显的弧岩浆特征。美国 Oregon 中新世(8 Ma)高铝橄榄拉斑玄武岩也具有亏损 Nb-Ta-Ti 和富集

表2 全部的 CFB、CRB、WPB 样品的主要元素($\times 10^{-6}$)、微量元素、稀土元素($\times 10^{-6}$)和同位素含量表
Table 2 Major element ($\text{wt}\%$), rare earth element ($\times 10^{-6}$) and isotope contents table from all the CFB, CRB and WPB

玄武岩	CFB			CRB			WPB								
	数据量	平均数	中位数	众数	主要分布范围	数据量	平均数	中位数	众数	主要分布范围	数据量	平均数	中位数	众数	主要分布范围
SiO ₂	14287	50.36	50.31	49.70	45~55	14690	49.45	49.22	48.00	45~55	4499	48.86	48.59	46.10	45~55
TiO ₂	14237	2.02	1.89	1.06	0.2~4.54	14660	1.84	1.88	2.20	0.1~4.08	4408	2.19	2.13	2.00	0.1~4.43
Al ₂ O ₃	14242	14.35	14.26	14.20	11.09~17.55	14631	15.23	15.11	14.00	10.35~20	4362	15.52	15.53	16.00	11.61~19.44
FeO ^r	9732	11.88	11.79	11.70	7.01~16.77	5097	9.99	10.01	10.80	3.62~16.37	4388	10.82	10.78	10.80	6.56~15.07
MgO	14268	6.01	5.92	4.90	1.72~10.3	14734	6.48	6.46	6.40	0.11~12.84	4393	6.50	6.53	4.70	1.22~11.72
MnO	13919	0.19	0.19	0.18	0.11~0.27	14479	0.16	0.16	0.17	0.07~0.26	4166	0.18	0.18	0.18	0.10~0.26
CaO	14244	9.60	9.76	9.76	5.67~12	14638	8.50	8.64	8.50	4.01~12	4346	9.27	9.32	8.80	5.14~11.99
Na ₂ O	14225	2.59	2.54	2.40	1.23~3.98	14741	3.33	3.29	3.10	1.12~5.58	4372	3.31	3.29	2.70	1.53~5.11
K ₂ O	14201	0.80	0.71	0.50	0.01~2.31	14965	1.39	1.25	1.00	0.001~4.1	4364	1.17	1.10	1.00	0.01~3.22
P ₂ O ₅	14067	0.26	0.23	0.16	0.01~0.68	14203	0.45	0.41	0.20	0.01~1.23	4308	0.46	0.43	0.20	0.01~1.17
Cs	2664	0.60	0.43	0.20	0.001~2.25	4852	0.85	0.55	0.20	0.01~3.75	961	0.38	0.32	0.20	0.01~1.3
Rb	11148	19.19	16.00	12.00	0.08~61	13777	32.21	25.09	15.00	0.01~111.8	3402	23.92	21.14	17.00	0.1~71
Ba	11243	275.2	219.0	160.0	1.01~884	12486	435.7	368.0	280.0	0.23~1422	3019	446.5	404.0	350.0	1.01~1201
Th	7129	2.68	2.25	3.00	0.08~8.22	10573	4.07	3.30	3.00	0.01~13.65	2306	3.70	3.27	4.00	0.02~10.6
U	4481	0.65	0.56	1.00	0.01~1.98	8421	1.03	0.90	1.00	0.01~3.25	1531	1.06	0.95	1.00	0.02~2.9
Nb	10081	11.89	10.20	10.00	1~32.9	11832	27.54	19.50	6.00	0.1~101	2877	32.23	26.00	9.00	0.3~110
Ta	4818	0.82	0.65	0.60	0.03~2.57	7880	1.68	1.20	0.30	0.01~6	1740	2.24	1.90	2.00	0.01~7
La	8432	17.31	15.00	12.00	0.1~48	11208	27.47	23.30	15.00	0.28~85.2	2805	30.11	27.50	25.00	0.24~83.98
Ce	8351	39.00	34.00	21.00	1~103	11170	56.94	49.80	31.00	0.52~166.19	2749	63.32	58.23	51.00	0.5~164
Pb	5040	4.39	3.99	5.00	0.05~13.8	8007	5.91	4.50	4.00	0.01~20.76	1350	4.76	4.00	6.00	0.2~13.7
Pr	3662	5.05	4.26	2.90	0.36~13.4	7352	7.13	6.43	12.00	0.16~19.44	940	8.44	8.05	10.00	0.13~19.8
Mo	480	1.09	1.07	0.70	0.1~2.5	962	1.90	1.50	2.00	0.05~6.1	47	1.87	1.15	0.44	0.24~6.2
Sr	11748	269.9	247.0	200.0	0.45~584	14136	554.4	516.0	530.0	0.28~1543	3531	531.4	497.0	104.0	0.16~1320
Nd	6705	21.18	18.62	12.00	1.1~52.49	11529	28.97	26.30	25.00	0.34~76.74	2363	32.93	30.80	30.00	0.29~76.9
Sm	6117	5.35	4.80	4.10	0.52~12.1	11030	6.16	5.85	5.00	0.1~14.14	2365	6.84	6.50	5.80	0.27~14.7
Zr	11521	147.1	138.0	140.0	0.18~328	12784	178.7	168.4	140.00	0.05~435	3364	187.8	178.0	125.0	1~418
Hf	5110	3.75	3.41	2.90	0.1~8.51	8665	4.34	4.13	4.00	0.1~9.95	1885	4.60	4.40	4.00	0.2~9.8
Eu	5853	1.72	1.56	1.40	0.17~3.72	9983	1.94	1.87	1.50	0.02~4.15	2200	2.18	2.10	2.10	0.12~4.4
Gd	4363	5.66	5.20	4.50	0.1~12.05	8332	5.81	5.69	6.00	0.33~11.7	1193	6.74	6.51	5.70	1.38~12.12
Tb	5284	0.92	0.86	0.80	0.09~1.85	8909	0.87	0.86	0.80	0.16~1.6	1886	0.97	0.95	0.70	0.14~1.81
Dy	3958	5.34	5.04	4.00	0.61~10.06	8089	4.75	4.65	4.60	1.32~8.29	1147	5.56	5.36	5.00	1.24~9.9
Li	861	8.27	7.98	5.00	0.11~20.9	1641	11.24	9.00	8.00	0.8~30.43	197	7.97	7.18	7.00	1.40~20.14
Y	11107	31.21	30.00	27.00	8.7~55.75	12247	24.87	24.00	22.00	6.2~44.37	2997	29.52	28.50	30.00	8~51.31
Ho	3481	1.08	1.04	0.80	0.22~1.96	7627	0.90	0.87	0.80	0.26~1.57	917	1.07	1.03	1.00	0.38~1.78
Er	3913	2.88	2.76	2.30	0.78~5.08	8018	2.37	2.28	2.00	0.58~4.21	1111	2.76	2.69	2.60	0.95~4.63
Tm	3283	0.41	0.40	0.36	0.1~0.74	6880	0.34	0.31	0.30	0.07~0.62	700	0.38	0.38	0.40	0.13~0.64
Yb	5909	2.65	2.57	3.00	0.72~4.63	9887	2.06	1.94	1.90	0.19~4	2150	2.43	2.36	2.20	0.76~4.17
Lu	5721	0.40	0.38	0.30	0.11~0.7	9554	0.30	0.29	0.30	0.03~0.62	2049	0.37	0.35	0.30	0.1~0.64
¹⁴³ Nd/ ¹⁴⁴ Nd	1985	0.51257	0.512568	0.51248	0.51181~0.513183	5520	0.70504	0.704489	0.7042	0.70171~0.71076	979	0.51276	0.512808	0.51295	0.51209~0.51337
⁸⁷ Sr/ ⁸⁶ Sr	2360	0.705973	0.70565	0.704	0.7018~0.71233	5241	0.512667	0.51273	0.5128	0.70171~0.71076	1147	0.704362	0.70393	0.70369	0.702~0.70809
²⁰⁶ Pb/ ²⁰⁴ Pb	1269	18.3648	18.42	17.93	16.542~20.154	2392	18.5589	18.66	18.573	16.851~20.2773	626	18.958	18.9864	18.93	17.324~20.428
²⁰⁷ Pb/ ²⁰⁴ Pb	1268	15.5517	15.566	15.53	15.215~15.872	2392	15.5809	15.594	15.61	15.341~15.81	626	15.6021	15.6	15.66	15.424~15.784
²⁰⁸ Pb/ ²⁰⁴ Pb	1269	38.4342	38.43	38.37	36.915~39.055	2394	38.5762	38.67	38.85	36.71~40.3342	626	38.8797	38.88	38.8	37.553~40.19

注:计算先采用箱型图去除异常值,只保留Q1(下四分位数)-1.5IQR(四分位距)到Q3(上四分位数)+1.5IQR之间的数据,然后求其平均值、中位数和众数当数据量为奇数时,处于中间位置的数据值为中位数;当数据量为偶数时,处于中间位置的2个数值的平均数当数据量为偶数时,处于中间位置的数据值为中位数

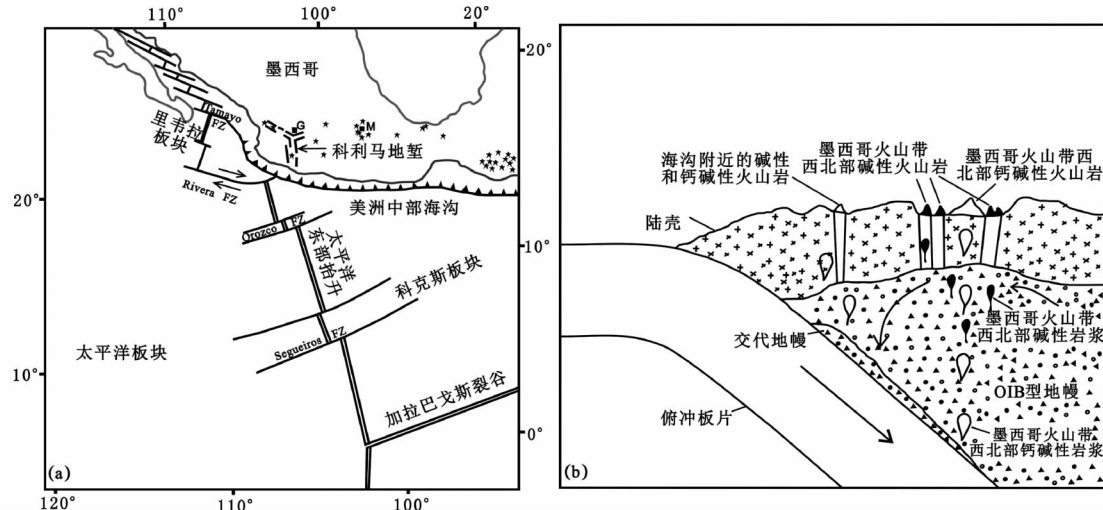


图 5 墨西哥西部科利马地堑位置图(a, 引自 Allan and Carmichael, 1984 的图 1)及裂谷形成示意图(b, 引自 Verma and Nelson, 1989 的图 11)

Fig. 5 Colima graben location map (a, after the Fig. 1 of Allan and Carmichael, 1984) and rift valley form diagram (b, after the Fig. 11 of Verma and Nelson, 1989) in western Mexico

Sr-Nd-Pb 同位素的特征,被认为是具有陆壳的特征,暗示了存在浅部地壳物质的再循环(Kelemen *et al.*, 1993; Plank, 2005)。据对北大西洋第三纪大火成岩省的研究,渐新世的 British Isles 熔岩是亏损 Nb 的,Fitton *et al.* (1997) 和 Kent and Fitton(2000)认为其来自一个 N-MORB 的源区。格陵兰东南沿海的裂谷玄武岩也是亏损 Zr、Nb、Ti 的,被认为是来自亏损的地幔源岩(Philipp *et al.*, 2001; Larsen *et al.*, 1999)。Greene *et al.* (2009)对加拿大 Yukon 地区三叠纪的大陆溢流玄武岩研究表明,低 Ti 玄武岩明显亏损 Nb 等 HFSE,推测其与消减带物质的带入有关(Pearce, 2008)。在冰岛和格陵兰地区,低 Ti 熔岩通常被认为是来自亏损的 MORB 源区 (Ellam and Stuart, 2000)。Soager and Holm (2011)对冰岛 Faroe 溢流玄武岩的研究表明,那里存在类似大西洋 MORB 的低钛玄武岩,暗示有来自上地幔的组分的加入。低钛玄武岩的地球化学特征类似 MORB,不同于占主导地位的高钛玄武岩。稀土元素指示其来源于比 N-MORB 更加亏损的源区,推测是尖晶石相和石榴石相地幔经历多次熔融的结果(Larsen *et al.*, 1999b; Callegaro *et al.*, 2013)。

(7) 贫 Ti 大陆裂谷玄武岩。大陆裂谷的形成通常与地幔隆升、岩石圈伸展作用有关,故有主动裂谷和被动裂谷之分。裂谷作用形成的典型岩石主要为拉斑玄武岩、碱性玄武岩以及与其相伴的中酸性岩组合共同组成的双峰式火山岩系列。在裂谷早期阶段,一般发育以碱性玄武岩为主的岩石组合,随着裂谷的拉伸,软流圈进一步发展,大陆最终被拉开有新洋壳形成时,可形成大量的拉斑玄武岩。然而,在 GEOROC 数据库中,裂谷构造背景下形成的岩石却不乏具有 MORB 以及 IAB 特征的低 Ti 玄武岩。由此可见,裂谷玄武岩的源区及岩浆作用的过程具有高度的不均一性。例如,美国

加利福尼亚和内华达大盆地西部的玄武岩,明显富集大离子亲石元素和亏损高场强元素,在微量元素蛛网图中出现 Nb-Ta负异常,暗示玄武岩岩浆源区受到来自俯冲带岩石圈的影响(Davis and Hawkesworth, 1995);新特提斯洋在二叠纪拉开的裂谷阶段出现三组岩浆系列:第一组是低Ti拉班玄武岩;第二组是碱性玄武岩,类似OIB的特征;第三组是由拉班玄武岩和碱性玄武岩交替组成,第一组低钛玄武岩的源岩被认为是来自亏损和富集地幔的混合(Lapierre et al., 2004);埃塞俄比亚Afar低钛玄武岩可能与东非裂谷地幔柱组分中再循环的古老洋壳有关(Barrat et al., 2003);墨西哥古近纪晚期和第四纪裂谷玄武岩,即是在太平洋板块向东消减时在消减带上盘形成的(Verma and Nelson, 1989; Allan and Carmichael, 1984; Wallace and Carmichael, 1992; Nelson and Carmichael, 1984; Orozco-Esquivel et al., 2007; Hasenaka et al., 1994; Siebe et al., 2004);加拿大纽芬兰奥陶纪的Wild Bight组火山岩具有岛弧的地球化学痕迹,被认为是在岛弧背景上伸展作用下形成的(Swinden et al., 1990)。因此,许多研究者认为,低钛玄武岩可能是在裂谷阶段受到来自消减带物质的影响(Köhler et al., 2009; West et al., 2004; Davis and Hawkesworth, 1995; Camiré et al., 1995; Cousens, 1996; Gazel et al., 2012; Verma and Nelson, 1989; Wallace and Carmichael, 1992; Orozco-Esquivel et al., 2007; Siebe et al., 2004),有点类似弧后盆地形成的模式(West et al., 2004; Gazel et al., 2012; Verma and Nelson, 1989)(图5)。

上述的实例表明，陆内玄武岩均表现出成分及成因的多样性，反映出其源区组分的变异性及不均一性，以及岩浆形成、演化过程中的影响因素的复杂性。早先建立的构造判别图就显得过于简单化和理想化。因此，我们应基于 GEOROC

数据库这个平台,对岩石分析数据进行科学的、严谨的筛选,采用数理统计的方法优选出最佳的元素组合及判别标准,结合地质实际,构建新的构造环境判别图。运用数理统计的方法将GEOROC数据库中筛选后的数据由低维向高维选择不同维度的数据组合,总结不同类型玄武岩元素的特征,选取有效的判别元素,构建高置信度的各类玄武岩构造判别的最优元素组合及分类标准,完善玄武岩构造判别图的理论与实践,提升岩石构造的研究水平。

5 结论

(1) 全体数据在早先的构造判别图上的投图结果表明,CFB、CRB、WPB几乎落入了各种玄武岩构造环境域,在有些判别图上大部分样品甚至落入MORB和岛弧区,而不是落入WPB区,说明许多玄武岩判别图的判别功能值得商榷,尤其是若干主元素判别图。

(2) CFB、CRB、WPB的源区复杂多样,有强烈富集的,也有亏损的。富集型玄武岩可能来自富集的下地幔,而亏损的玄武岩来自具有MORB或岛弧特征的软流圈地幔,后者表现为明显亏损Nb-Ta为特征。低钛玄武岩大多是亏损或强烈亏损的,而高钛玄武岩则通常是富集型的。低程度部分熔融、在较浅深度的部分熔融、结晶分离作用、陆壳混染作用以及AFC过程亦可形成Nb-Ta亏损的大陆玄武岩,尤其是低钛玄武岩。

(3) 大量数据的挖掘研究表明,各种构造环境下形成的玄武岩均表现出成分及成因的多样性,反映出其源区组分的变异性和平匀性,以及岩浆形成、演化过程中的影响因素的复杂性。因此,早先建立的构造判别图就显得过于简单化和理想化。鉴此,我们在研究岩石形成的构造背景及其地球动力学过程时,应注重岩石地球化学特征与其源区、岩浆作用过程的内因外因的成因联系,注重岩石组合在野外产出的时空关系,紧密结合野外地质实际及区域大地构造演化史,之后对岩石形成的构造动力学过程作出合理的解释。

(4) 尽管从全体数据的研究中发现早先的判别图存在许多缺陷,但也不能因此而全盘否定判别图的理论和方法,判别图毕竟还有其合理的内核。因此,我们应基于GEOROC数据库这个平台,对岩石分析数据进行严谨的筛选,采用数理统计的方法优选出最佳的元素组合及判别标准,结合地质实际,构建新的构造环境判别图。

致谢 本文成文过程中得到张岱、苗秀全、杜君和杜雪亮同学的帮助,特别是三位匿名审稿人对本文的评论和建议,使文章质量得以提高,在此深表感谢!

References

Allan JF and Carmichael ISE. 1984. Lamprophyric lavas in the Colima

- graben, SW Mexico. Contributions to Mineralogy and Petrology, 88(3): 203–216
- Arndt NT and Christensen U. 1992. The role of lithospheric mantle in continental flood volcanism: Thermal and geochemical constraints. Journal of Geophysical Research, 97(B7): 10967–10981
- Arndt NT, Czamanske GK, Wooden JL and Fedorenko VA. 1993. Mantle and crustal contributions to continental flood volcanism. Tectonophysics, 223(1–2): 39–52
- Barrat JA, Joron JL, Taylor RN, Fourcade S, Nesbitt RW and Jahn BM. 2003. Geochemistry of basalts from Manda Hararo, Ethiopia: LREE-depleted basalts in Central Afar. Lithos, 69(1–2): 1–13
- Best MG and Christiansen EH. 2001. Igneous Petrology. Malden, MA: Blackwell Science
- Cabanis B and Lecolle M. 1989. Le diagramme La/10-Y/15-Nb/8: Un outil pour la discrimination des séries volcaniques et la mise en évidence des processus de mélange et/ou de contamination crustale. Comptes Rendus de l'Académie des Sciences. Série 2, 309(20): 2023–2029
- Callegaro S, Marzoli A, Bertrand H, Chiaradia M, Reisberg L, Meyzen C, Bellieni G, Weems RE and Merle R. 2013. Upper and lower crust recycling in the source of CAMP basaltic dykes from southeastern North America. Earth and Planetary Science Letters, 376: 186–199
- Camiré G, La Flèche MR and Jenner GA. 1995. Geochemistry of pre-Taconian mafic volcanism in the Humber Zone of the northern Appalachians, Québec, Canada. Chemical Geology, 119(1–4): 55–77
- Campbell IH and Griffiths RW. 1990. Implications of mantle plume structure for the evolution of flood basalts. Earth and Planetary Science Letters, 99(1–2): 79–93
- Capedri S, Venturelli G, Bocchi G, Dostal J, Garuti G and Rossi A. 1980. The geochemistry and petrogenesis of an ophiolitic sequence from Pindos, Greece. Contributions to Mineralogy and Petrology, 74(2): 189–200
- Cornell DH, Thomas RJ, Bowring SA, Armstrong RA and Grantham GH. 1996. Protolith interpretation in metamorphic terranes: A back-arc environment with Besshi-type base metal potential for the Quha Formation, Natal Province, South Africa. Precambrian Research, 77(3–4): 243–271
- Cousens BL. 1996. Magmatic evolution of Quaternary mafic magmas at Long Valley Caldera and the Devils Postpile, California: Effects of crustal contamination on lithospheric mantle-derived magmas. Journal of Geophysical Research: Solid Earth, 101(B12): 27673–27689
- Cox KG, Macdonald R and Hormung G. 1967. Geochemical and petrographic provinces in the Karroo basalts of Southern Africa. American Mineralogist, 52: 1451–1474
- Davis JM and Hawkesworth CJ. 1995. Geochemical and tectonic transitions in the evolution of the Mogollon-Datil Volcanic Field, New Mexico, U.S.A. Chemical Geology, 119(1–4): 31–53
- Deckart K, Bertrand H and Liégeois JP. 2005. Geochemistry and Sr, Nd, Pb isotopic composition of the Central Atlantic Magmatic Province (CAMP) in Guyana and Guinea. Lithos, 82(3–4): 289–314
- DeMin A, Piccirillo EM, Marzoli A, Bellieni G, Renne PR, Ernesto M and Marques L. 2003. The Central Atlantic Magmatic Province (CAMP) in Brazil: Petrology, Geochemistry, $^{40}\text{Ar}/^{39}\text{Ar}$ ages, paleomagnetism and geodynamic implications. In: Hames WE, McHome JG, Renne PR and Ruppel C (eds.). The Central Atlantic Magmatic Province: Insights from Fragments of Pangea. New York: American Geophysical Union, 136: 209–226
- Deng JF, Liu C, Feng YF, Xiao QH, Di YJ, Su SG, Zhao GC, Duan PX and Dai M. 2015. On the correct application in the common igneous petrological diagrams: Discussion and suggestion. Geological Review, 61(4): 717–734 (in Chinese with English abstract)
- Dorais MJ and Tubrett M. 2008. Identification of a subduction zone component in the Higganum dike, Central Atlantic Magmatic province: A LA-ICPMS study of clinopyroxene with implications for

- flood basalt petrogenesis. *Geochemistry, Geophysics, Geosystems*, 9 (10), doi: 10.1029/2008GC002079
- Dunning GR, Swinden HS, Kean BF, Evans DTW and Jenner GA. 1991. A Cambrian island arc in Iapetus: Geochronology and geochemistry of the Lake Ambrose volcanic belt, Newfoundland Appalachians. *Geological Magazine*, 128(1): 1–17
- Eglington BM, Harmer RE and Kerr A. 1989. Isotope and geochemical constraints on Proterozoic crustal evolution in South-East Africa. *Precambrian Research*, 45(1–3): 159–174
- Eglington BM and Armstrong RA. 2003. Geochronological and isotopic constraints on the Mesoproterozoic Namaqua-Natal Belt: Evidence from deep borehole intersections in South Africa. *Precambrian Research*, 125(3–4): 179–189
- Elburg M and Goldberg A. 2000. Age and geochemistry of Karoo dolerite dykes from Northeast Botswana. *Journal of African Earth Sciences*, 31(3–4): 539–554
- Ellam RM and Cox KG. 1991. An interpretation of Karoo picrite basalts in terms of interaction between asthenospheric magmas and the mantle lithosphere. *Earth and Planetary Science Letters*, 105(1–3): 330–342
- Ellam RM and Stuart FM. 2000. The sub-lithospheric source of North Atlantic basalts: Evidence for, and significance of, a common end-member. *Journal of Petrology*, 41(7): 919–932
- Fitton JG, Saunders AD, Norry MJ, Hardarson BS and Taylor RN. 1997. Thermal and chemical structure of the Iceland plume. *Earth and Planetary Science Letters*, 153(3–4): 197–208
- Gallagher K and Hawkesworth C. 1992. Dehydration melting and the generation of continental flood basalts. *Nature*, 358(6381): 57–59
- Gallagher K and Hawkesworth C. 1994. Mantle plumes, continental magmatism and asymmetry in the South Atlantic. *Earth and Planetary Science Letters*, 123(1–3): 105–117
- Galoyan G, Rolland Y, Sosson M, Corsini M and Melkonyan R. 2007. Evidence for superposed MORB, oceanic plateau and volcanic arc series in the Lesser Caucasus (Stepanavan, Armenia). *Comptes Rendus Geoscience*, 339(7): 482–492
- Gazel E, Plank T, Forsyth DW, Bendersky C, Lee CTA and Hauri EH. 2012. Lithosphere versus asthenosphere mantle sources at the Big Pine Volcanic Field, California. *Geochemistry, Geophysics, Geosystems*, 13(6), doi: 10.1029/2012GC004060
- Gibson SA, Thompson RN, Dickin AP and Leonards OH. 1995. High-Ti and low-Ti mafic potassic magmas: Key to plume-lithosphere interactions and continental flood-basalt genesis. *Earth and Planetary Science Letters*, 136(3–4): 149–165
- Gibson SA, Thompson RN, Dickin AP and Leonards OH. 1996. Erratum to “High-Ti and low-Ti mafic potassic magmas: Key to plume-lithosphere interactions and continental flood-basalt genesis” [Earth Planet. Sci. Lett. 136 (1995) 149–165]. *Earth and Planetary Science Letters*, 141(1–4): 325–341
- Gibson SA, Thompson RN and Day JA. 2006. Timescales and mechanisms of plume-lithosphere interactions: $^{40}\text{Ar}/^{39}\text{Ar}$ geochronology and geochemistry of alkaline igneous rocks from the Paraná-Etendeka large igneous province. *Earth and Planetary Science Letters*, 251(1–2): 1–17
- Glassley WE. 1974. Geochemistry and tectonics of the Crescent volcanic rocks, Olympic Peninsula, Washington. *Geological Society of America Bulletin*, 85(5): 785–794
- Greene AR, Scoates JS, Weis D and Israel S. 2009. Geochemistry of Triassic flood basalts from the Yukon (Canada) segment of the accreted Wrangellia oceanic plateau. *Lithos*, 110(1–4): 1–19
- Harris NBW, Pearce JA and Tindle AG. 1986. Geochemical characteristics of collision-zone magmatism. In: Coward MP and Ries AC (eds.). *Collision Tectonics*. Geological Society, London, Special Publications, 19(1): 67–81
- Hasenaka Y, Ban M and Granados HD. 1994. Contrasting volcanism in the Michoacán-Guanajuato volcanic field, central Mexico: Shield volcanoes vs. cinder cones. *Geofísica Internacional*, 33(1): 125–138
- Hawkesworth CJ, Marsh JS, Duncan AR, Erlank AJ and Norry MJ. 1984. The role of continental lithosphere in the generation of the Karoo volcanic rocks: Evidence from combined Nd- and Sr-isotope studies. In: Erlank AJ (eds.). *Petrogenesis of the Volcanic Rocks of the Karoo Province*. The Geological Society of South Africa, 13: 341–354
- Hawkesworth CJ, Mantovani M and Peate D. 1988. Lithosphere remobilization during Paraná CFB magmatism. *Journal of Petrology*, 1(1): 205–223
- Heinonen JS, Carlson RW and Luttmann AV. 2010. Isotopic (Sr, Nd, Pb and Os) composition of highly magnesian dikes of Vestfjella, western Dronning Maud Land, Antarctica: A key to the origins of the Jurassic Karoo large igneous province? *Chemical Geology*, 277(3–4): 227–244
- Huang YM, Van Calsteren P and Hawkesworth CJ. 1995. The evolution of the lithosphere in southern Africa: A perspective on the basic granulite xenoliths from kimberlites in South Africa. *Geochimica et Cosmochimica Acta*, 59(23): 4905–4920
- Kampunzu AB, Tombale AR, Zhai M, Bagai Z, Majaula T and Modisi MP. 2003. Major and trace element geochemistry of plutonic rocks from Francistown, NE Botswana: Evidence for a Neoarchaean continental active margin in the Zimbabwe craton. *Lithos*, 71(2–4): 431–460
- Kelemen PB, Shimizu N and Dunn T. 1993. Relative depletion of niobium in some arc magmas and the continental crust: Partitioning of K, Nb, La and Ce during melt/rock reaction in the upper mantle. *Earth and Planetary Science Letters*, 120(3–4): 111–134
- Kent RW and Fitton JG. 2000. Mantle sources and melting dynamics in the British Palaeogene Igneous Province. *Journal of Petrology*, 41(7): 1023–1040
- Kerr AC and Mahoney JJ. 2007. Oceanic plateaus: Problematic plumes, potential paradigms. *Chemical Geology*, 241(3–4): 332–353
- Köhler J, Schönenberger J, Upton B and Markl G. 2009. Halogen and trace-element chemistry in the Gardar Province, South Greenland: Subduction-related mantle metasomatism and fluid exsolution from alkalic melts. *Lithos*, 113(3–4): 731–747
- Lana C, Reimold WU, Gibson RL, Koeberl C and Siegesmund S. 2004. Nature of the Archean midcrust in the core of the Vredefort Dome, Central Kaapvaal Craton, South Africa. *Geochimica et Cosmochimica Acta*, 68(3): 623–642
- Lapierre H, Samper A, Bosch D, Maury RC, Béchenec F, Cotten J, Demant A, Brunet P, Keller F and Marcoux J. 2004. The Tethyan plume: Geochemical diversity of Middle Permian basalts from the Oman rifted margin. *Lithos*, 74(3–4): 167–198
- Larsen LM, Waagstein R, Pedersen AK and Storey M. 1999a. Trans-Atlantic correlation of the Palaeogene volcanic successions in the Faeroe Islands and East Greenland. *Journal of the Geological Society*, 156(6): 1081–1095
- Larsen LM, Fitton JG and Saunders AD. 1999b. Composition of volcanic rocks from the Southeast Greenland Margin, Leg 163: Major and trace element geochemistry. *Proceedings of the Ocean Drilling Program*, 163: 63–75
- Li C, Arndt NT, Tang QY and Ripley EM. 2015. Trace element indiscrimination diagrams. *Lithos*, 232: 76–83
- Luttmann AV and Furnes H. 2000. Flood basalts of Vestfjella: Jurassic magmatism across an Archaean-Proterozoic lithospheric boundary in Dronning Maud Land, Antarctica. *Journal of Petrology*, 41(8): 1271–1305
- Marsh JS, Hooper PR, Rehacek J, Duncan RA and Duncan AR. 1997. Stratigraphy and age of the Karoo basalts of Lesotho and implications for correlations within the Karoo igneous province. In: Mahoney JJ and Coffin MF (eds.). *Large Igneous Provinces: Continental, Oceanic, and Planetary Flood Volcanism*. New York: American Geophysical Union, 100: 247–272
- Maxeiner RO, Corrigan D, Harper CT, MacDougall DG and Ans dell K. 2005. Paleoproterozoic arc and ophiolitic rocks on the northwest margin of the Trans-Hudson Orogen, Saskatchewan, Canada: Their contribution to a revised tectonic framework for the orogeny. *Precambrian Research*, 136(1): 67–106

- Meschede M. 1986. A method of discriminating between different types of mid-ocean ridge basalts and continental tholeiites with the Nb-Zr-Y diagram. *Chemical Geology*, 56(3–4): 207–218
- Mullen ED. 1983. MnO/TiO₂/P₂O₅: A minor element discriminant for basaltic rocks of oceanic environments and its implications for petrogenesis. *Earth and Planetary Science Letters*, 62(1): 53–62
- Nelson SA and Carmichael ISE. 1984. Pleistocene to recent alkalic volcanism in the region of Sanganguey volcano, Nayarit, Mexico. *Contributions to Mineralogy and Petrology*, 85(4): 321–335
- Orozco-Esquivel T, Petrone CM, Ferrari L, Tagami T and Manetti P. 2007. Geochemical and isotopic variability in lavas from the eastern Trans-Mexican Volcanic Belt: Slab detachment in a subduction zone with varying dip. *Lithos*, 93(1–2): 149–174
- Pearce JA and Cann JR. 1973. Tectonic setting of basic volcanic rocks determined using trace element analyses. *Earth and Planetary Science Letters*, 19(2): 290–300
- Pearce JA. 1975. Basalt geochemistry used to investigate past tectonic environments on Cyprus. *Tectonophysics*, 25(1–2): 41–67
- Pearce JA. 1976. Statistical analysis of major element patterns in basalts. *Journal of Petrology*, 17(1): 15–43
- Pearce JA and Gale GH. 1977. Identification of ore-deposition environment from trace-element geochemistry of associated igneous host rocks. In: *Volcanic Processes in Ore Genesis*. Geological Society, London, Special Publications, 7: 14–24
- Pearce JA and Norry MJ. 1979. Petrogenetic implications of Ti, Zr, Y, and Nb variations in volcanic rocks. *Contributions to Mineralogy and Petrology*, 69(1): 33–47
- Pearce JA, Alabaster T, Shelton AW and Searle MP. 1981. The Oman ophiolite as a Cretaceous arc-basin complex: Evidence and implications. *Philosophical Transactions of the Royal Society A: Mathematical, Physical and Engineering Sciences*, 300(1454): 299–317
- Pearce JA. 1982. Trace element characteristics of lavas from destructive plate boundaries. In: Thorpe RS (ed.). *Orogenic Andesites and Related Rocks*. Chichester, England: John Wiley and Sons, 525–548
- Pearce JA. 1983. Role of the sub-continental lithosphere in magma genesis at active continental margins. In: Hawkesworth CJ and Norry MJ (eds.). *Continental Basalts and Mantle Xenoliths*. Nantwich, Cheshire: Shiva Publications, 230–249
- Pearce JA, Lippard SJ and Roberts S. 1984. Characteristics and tectonic significance of supra-subduction zone ophiolites. In: Gass IG, Lippard SJ and Shelton AW (eds.). *Ophiolites and Oceanic Lithosphere*. Geological Society, London, Special Publications, 16: 77–94
- Pearce JA and Peate DW. 1995. Tectonic implications of the composition of volcanic arc magmas. *Annual Review of Earth and Planetary Sciences*, 23(1): 251–285
- Pearce JA and Robinson RB. 2000. *Strategic Management: Formulation, Implementation and Control*. 7th Edition. Boston: Irwin/McGraw-Hill
- Pearce JA. 2008. Geochemical fingerprinting of oceanic basalts with applications to ophiolite classification and the search for Archean oceanic crust. *Lithos*, 100(1–4): 14–48
- Peate DW and Hawkesworth CJ. 1996. Lithospheric to asthenospheric transition in low-Ti flood basalts from southern Parana, Brazil. *Chemical Geology*, 127(1–3): 1–24
- Petrini R, Civetta L, Piccirillo EM, Bellieni G, Comin-Chiaromonti P, Marques LS and Melfi AJ. 1987. Mantle heterogeneity and crustal contamination in the genesis of low-Ti continental flood basalts from the Paraná plateau (Brazil): Sr-Nd isotope and geochemical evidence. *Journal of Petrology*, 28(4): 701–726
- Philipp H, Eckhardt JD and Puchelt H. 2001. Platinum-group elements (PGE) in basalts of the seaward-dipping reflector sequence, SE Greenland coast. *Journal of Petrology*, 42(2): 407–432
- Piccirillo EM, Civetta L, Petrini R, Longinelli A, Bellieni G, Comin-Chiaromonti P, Marques LS and Melfi AJ. 1989. Regional variations within the Paraná flood basalts (southern Brazil): Evidence for subcontinental mantle heterogeneity and crustal contamination. *Chemical Geology*, 75(1–2): 103–122
- Plank T. 2005. Constraints from thorium/lanthanum on sediment recycling at subduction zones and the evolution of the continents. *Journal of Petrology*, 46(5): 921–944
- Puffer JH. 2001. Contrasting high field strength element contents of continental flood basalts from plume versus reactivated-arc sources. *Geology*, 29(8): 675–678
- Rogers N, van Staal CR, McNicoll V, Pollock J, Zagorevski A and Whalen J. 2006. Neoproterozoic and Cambrian arc magmatism along the eastern margin of the Victoria Lake Supergroup: A remnant of Ganderian basement in central Newfoundland? *Precambrian Research*, 147(3–4): 320–341
- Rollinson HR. 1993. *Using Geochemical Data: Evaluation, Presentation, Interpretation*. Harlow: Longman Scientific & Technical
- Shervais JW. 1982. Ti-V plots and the petrogenesis of modern and ophiolitic lavas. *Earth and Planetary Science Letters*, 59(1): 101–118
- Siebe C, Rodríguez-Lara V, Schaaf P and Abrams M. 2004. Geochemistry, Sr-Nd isotope composition, and tectonic setting of Holocene Pelado, Guespalapa and Chichinautzin scoria cones, south of Mexico City. *Journal of Volcanology and Geothermal Research*, 130(3–4): 197–226
- Snow CA. 2006. A reevaluation of tectonic discrimination diagrams and a new probabilistic approach using large geochemical databases: Moving beyond binary and ternary plots. *Journal of Geophysical Research: Solid Earth*, 111(B6), doi: 10.1029/2005JB003799
- Søager N and Holm PM. 2011. Changing compositions in the Iceland plume: Isotopic and elemental constraints from the Paleogene Faroe flood basalts. *Chemical Geology*, 280(3–4): 297–313
- Sun SS and McDonough WF. 1989. Chemical and isotopic systematics of oceanic basalts: Implications for mantle composition and processes. In: Saunders AD and Norry MJ (eds.). *Magma in the Ocean Basins*. Geological Society, London, Special Publications, 42: 313–345
- Swinden HS, Jenner GA, Fryer BJ, Hertogen J and Roddick JC. 1990. Petrogenesis and paleotectonic history of the Wild Bight Group, an Ordovician rifted island arc in central Newfoundland. *Contributions to Mineralogy and Petrology*, 105(2): 219–241
- Verma SP and Nelson SA. 1989. Isotopic and trace element constraints on the origin and evolution of alkaline and calc-alkaline magmas in the Northwestern Mexican Volcanic Belt. *Journal of Geophysical Research: Solid Earth*, 94(B4): 4531–4544
- Vermeesch P. 2006a. Tectonic discrimination of basalts with classification trees. *Geochimica et Cosmochimica Acta*, 70(7): 1839–1848
- Vermeesch P. 2006b. Tectonic discrimination diagrams revisited. *Geochemistry, Geophysics, Geosystems*, 7(6), doi: 10.1029/2005GC001092
- Wallace P and Carmichael SE. 1992. Alkaline and calc-alkaline lavas near Los Volcanes, Jalisco, Mexico: Geochemical diversity and its significance in volcanic arcs. *Contributions to Mineralogy and Petrology*, 111(4): 423–439
- Wang YJ, Zhao GC, Fan WM, Peng TP, Sun LH and Xia XP. 2007. LA-ICP-MS U-Pb zircon geochronology and geochemistry of Paleoproterozoic mafic dykes from western Shandong Province: Implications for back-arc basin magmatism in the Eastern Block, North China Craton. *Precambrian Research*, 154(1–2): 107–124
- West DP, Coish RA and Tomascak PB. 2004. Tectonic setting and regional correlation of Ordovician metavolcanic rocks of the Casco Bay Group, Maine: Evidence from trace element and isotope geochemistry. *Geological Magazine*, 141(2): 125–140
- Wilson M. 1997. Thermal evolution of the Central Atlantic passive margins: Continental break-up above a Mesozoic super-plume. *Journal of the Geological Society*, 154(3): 491–495
- Wood DA, Joron JL and Treuil M. 1979. A re-appraisal of the use of trace elements to classify and discriminate between magma series erupted in different tectonic settings. *Earth and Planetary Science Letters*, 45(2): 326–336

- Wood DA. 1980. The application of a Th-Hf-Ta diagram to problems of tectonomagmatic classification and to establishing the nature of crustal contamination of basaltic lavas of the British Tertiary Volcanic Province. *Earth and Planetary Science Letters*, 50(1) : 11 - 30
- Workman RK and Hart SR. 2005. Major and trace element composition of the depleted MORB mantle (DMM). *Earth and Planetary Science Letters*, 231(1 - 2) : 53 - 72
- Zhang ZC, Wang FS, Fan WM, Deng HL, Xu YG, Xu JF and Wang YJ. 2001. A discussion on some problems concerning the study of the Emeishan basalts. *Acta Petrologica et Mineralogica*, 20(3) : 239 - 246 (in Chinese with English abstract)
- Zindler A and Hart SR. 1986. Chemical geodynamics. *Annual Review of Earth and Planetary Sciences*, 14(1) : 493 - 571

Earth and Planetary Sciences, 14(1) : 493 - 571

附中文参考文献

- 邓晋福, 刘翠, 冯艳芳, 肖庆辉, 狄永军, 苏尚国, 赵国春, 段培新, 戴蒙. 2015. 关于火成岩常用图解的正确使用: 讨论与建议. 地质论评, 61(4) : 717 - 734
- 张招崇, 王福生, 范蔚茗, 邓海琳, 徐义刚, 许继峰, 王岳军. 2001. 峨眉山玄武岩研究中的一些问题的讨论. 岩石矿物学杂志, 20(3) : 239 - 246